DISTRIBUTION STATEMENT A: Distribution approved for public release; distribution is unlimited.

Dispersion in the Surfzone: Tracer Dispersion Studies

Dr. Falk Feddersen
Scripps Institutions of Oceanography
IOD/SIO/UCSD 0209, 9500 Gilman Drive, La Jolla CA 92093-0209
858.534.4345, 858.534.0300 (FAX), falk@coast.ucsd.edu
http://iod.ucsd.edu/∼falk

Award Number: N00014-06-1-0330

LONG-TERM GOALS

Terrestrial runoff and river input dominates urban pollutant loading rates degrading nearshore and surfzone water quality (*e.g., Boehm et al.*, 2002). Surfzone mixing processes disperse and dilute such (and other types of) pollution. On smaller length-scales (smaller than the water depth), breaking-waves and bed-generated turbulence mix tracer. However, field surfzone observations of turbulence previously have been extremely scarce, and much about surfzone small-scale turbulence is not known. On larger scales (10–100 m), horizontal dispersion is driven by surfzone eddies and meanders associated with shear waves (*Oltman-Shay et al.*, 1989) or finite breaking crest length (*Peregrine*, 1998). Understanding the small and large length-scale mixing processes important to predicting the fate (transport, dispersal, and dilution) of surfzone tracers whether pollution, bacteria, larvae, or nutrients.

OBJECTIVES

The scientific objective is to improve understanding and modeling of dispersion of tracers (pollution, fecal indicator bacteria, fine sediments) within the nearshore (a few 100 m of the shoreline) and the surfzone. In this report, the focus is on three research components built upon observations from the HB06 experiment (PIs: Feddersen and Guza). The first is stochastic modeling of surfzone drifter dispersion from the HB06 experiment (*Spydell and Feddersen*, 2011). Second, studying the small-scale turbulence in the surfzone due to breaking waves and bottom boundary layer processes (*Feddersen*, 2011). Third, is modeling nearshore nutrient fluxes and the resulting phytoplankton and comparing it to observations (*Omand et al.*, 2011b). In addition, IB09 experiment (performed in collaboration with R. T. Guza) analysis is ongoing and is not described here.

APPROACH

HB06 Dye Dispersion Modeling

A Boussinesq wave-current model *funwaveC* has been coupled with a tracer evolution model. The model reproduces the observed wave and current conditions on the 5 days of HB06 dye releases. Dye tracer is released in the model, and the model dye tracer transport and dispersion is

analyzed analogous to the observations (*e.g., Clark et al.*, 2010a). The results are presented in *Feddersen et al.* (2011) and *Clark et al.* (2011), and are not discussed further here.

Stochastic Particle Simulation for Surfzone Dispersion

Drifter-derived diffusivities are time-dependent. In an unbounded domain, diffusivities are monotonic with a linear ballistic regime for times $\ll$ the Lagrangian time-scale τ and become constant at times $\gg \tau$. For five HB06 experiment drifter release-days on an alongshore uniform beach, the cross-shore diffusivity K_x was estimated for times < 1000 s using an unbiased estimator (*Spydell et al.*, 2009). The estimated K_x had a ballistic regime for $t < 50$ s, a maximum around 100 s, with a slow decay for longer times. A potential reasons why a monotonic K_x may not be expected in the surfzone is the presence of a boundary of the beach which prevents unbounded diffusion. Here HB06 particle trajectories are stochastically simulated with the Langevin equations with a shoreline boundary to explain the observed features of the cross- and alongshore diffusivities The approach here was developed in collaboration with Project Scientist Matt Spydell.

Small-scale Surfzone Turbulence

The vertical structure of turbulence in the surfzone is of interest. Both breaking waves and near-sea-bed shear are possible sources of turbulence. Here a key turbulence statistic, the turbulent dissipation rate ϵ is estimated from Acoustic Doppler Velocimeters observations following *Feddersen et al.* (2007) and *Feddersen* (2010). The effect of both wave-breaking and bottom boundary layer processes (BBL) upon ϵ are examined.

Episodic Nutrient Fluxes and Phytoplankton Modeling

In Southern California, intense phytoplankton blooms localized in the nearshore (< 20 m depth) appear intermittently, particularly during summer and fall. The underlying drivers of these blooms are poorly understood. Three distinct phytoplankton blooms lasting 4–9 days were observed in approximately 15 m water depth near Huntington Beach CA between June - October of 2006 during the HB06 experiment. Vertical nutrient (nitrate) fluxes are parameterized and used to drive a nitrate-phytoplankton model. This work is part of former graduate student Melissa Omand's thesis.

WORK COMPLETED

- *Clark et al.* (2010a) of the HB06 dye dispersion studies has been published in JGR Oceans.
- A manuscript (*Feddersen*, 2010) has been published in *J. Atmospheric and Oceanic Tech.*. This manuscript deals with the methods of analyzing Acoustic Doppler Velocimeter data for estimating the turbulent dissipation rate in the surfzone and air-sea boundary regions
- *Omand et al.* (2011a) has been published in *Limnology and Oceanography*, reporting on the evolution and dynamics of a nearshore red tide observed during HB06.
- *Feddersen* (2011), on surfzone turbulence dynamics from HB06 observations, is press to JPO.

- *Spydell and Feddersen* (2011), on a theoretical analysis of finite-Lagrangian time-scale on shear dispersion is in press to JFM.
- A two-part paper series (*Clark et al.*, 2011; *Feddersen et al.*, 2011) on Boussinesq modeling of surfzone tracer dispersion is in press to JGR.
- A manuscript (*Spydell and Feddersen*, 2011) on stochastic simulation of surfzone particle dispersion is in preparation for JGR.
- Analysis of the IB09 (Imperial Beach CA in Sept-Oct 2009) experiment (PIs: Guza and Feddersen) is in full swing.

RESULTS

Background: HB06 Experiment

Observations were collected from 15 September to 17 October 2006 (800 hours) at Huntington Beach CA, a site with chronic water quality problems. A cross-shore transect of co-located pressure sensors and acoustic Doppler Velocimeters was deployed spanning 160 m out to 4 m mean water depth. The tide range was nominally ± 1 m. The data was sampled at 8 Hz. The ADVs sampled between 0.5-1.0 m above the bed. The cross- and alongshore coordinate are x and y, respectively. The mean water depth is given by h. At each of the frames, hourly estimates of significant wave height H_{sig}, mean alongshore current $\bar{v}$, and turbulent dissipation rate ϵ were estimated.

Stochastic Simulation of Surfzone Drifter Dispersion

An unusual feature of the HB06 cross-shore drifter diffusivities is their non-monotonic nature (they decrease with time). This behavior is explored by stochastic particle simulations governed by the Langevin equations. Please see *Spydell and Feddersen* (2011) for full details.

The results of the model simulations are shown in Figure 1. At short times ($t < 50$ s and $t/\tau_x < 0.7$) the modeled $K_x^{(\text{m})}$ and analytic $K_x^{(\text{h})}$ diffusivities reproduce well the observed $K_x^{(\text{o})}$ (compare the dashed, solid, and dash-dot curves in Figure 1, left column) as cross-dispersion is in a ballistic regime ($K_x = \sigma_u^2 t$). This also indicates that the bulk cross-shore velocity variance σ_u^2 used in the modeled and analytic solutions is accurate. With the exception of 10/14, the modeled $K_x^{(\text{m})}$ reproduces the observed $K_x^{(\text{o})}$ at longer times ($t > 400$ s or $t/\tau_x > 3$, left and right columns of Figure 1, respectively). Similarly, at longer times, the analytic $K_x^{(\text{h})}$ also reproduces $K_x^{(\text{o})}$ on 10/02 and 10/03, but somewhat underpredicts $K_x^{(\text{o})}$ on 09/17 and 10/15. As discussed in *Spydell et al.* (2009), the poor model prediction on 10/14 at longer times, drifter trajectories converged in the inner-mid surfzone suggesting bathymetric control and resulting in the rapid longer time decay in $K_x^{(\text{o})}$. For more information please see *Spydell and Feddersen* (2011).

Small-scale Surfzone Turbulence: Dissipation and Wave Energy Flux Relationship

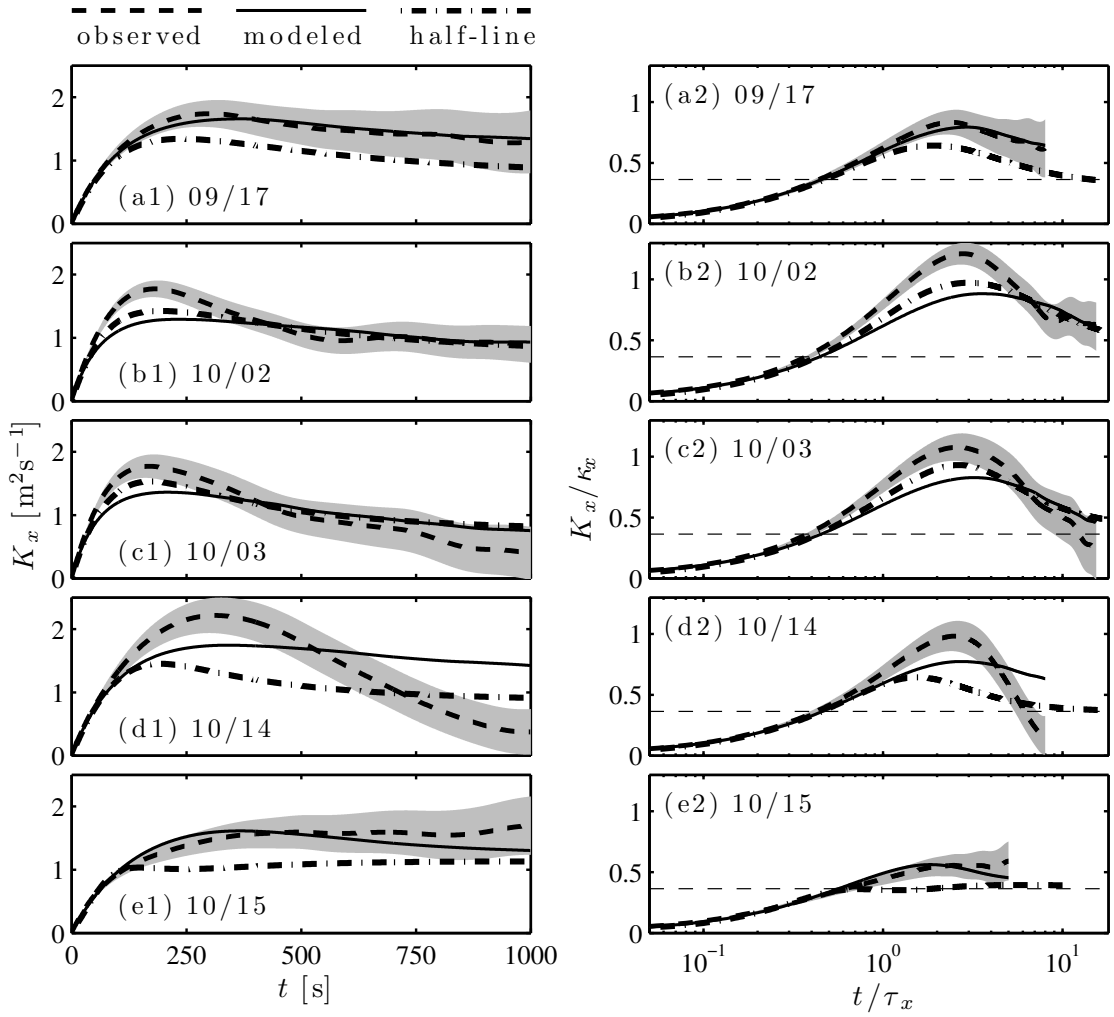

Figure 1: (left) The cross-shore diffusivity K_x versus time t and (right) the non-dimensionalized diffusivity K_x/κ_x versus t/τ_x for the 5 dye-release days (rows). In each panel the observed (dashed) and Langevin equation modeled (solid) and the analytic (dash-dot) are indicated by the legend. In all panels the shaded gray region represents the observed $K_x^{(\mathrm{o})}$ sampling error. In panels (a2)-(e2), the best-fit τ_x and and $\kappa_x = \sigma_u^2 \tau_x$ are used, and the analytic expression for the long-time $K_x/\kappa_x = (1 - 2/\pi) \approx 0.36$ is shown in the thin dashed line.

During the HB06 experiment, the turbulent dissipation rate ϵ typically was significantly larger (by a factor of 10) within the surfzone relative to seaward of the surfzone, suggesting the importance of wave breaking to surfzone turbulence. Waves approaching the surfzone have an associated onshore wave energy flux F that is conserved until wave breaking begins. As $F = 0$ at the shoreline, the incoming wave energy must be converted into other forms of energy within the surfzone. In the simplest steady-state energy balance, the incident wave energy flux is balanced by the depth-integrated turbulent dissipation over the entire surfzone. If dissipation were depth-uniform, then the simple cross-shore integrated energy balance between the incident wave energy flux and surfzone dissipation becomes

$$\int_0^{x_\mathrm{b}} h\epsilon \,\mathrm{d}x = F_{x_{\mathrm{F7}}}. \tag{1}$$

The dissipation rate ϵ varies over the vertical (*e.g.,* George et al., 1994), and surfzone laboratory experiments indicate the majority of dissipation occurs above trough level as found in laboratory studies.. Thus the assumption that $\int \epsilon(z)\mathrm{d}z = h\epsilon$ is not appropriate. However the observed $h\epsilon$ likely is proportional to the depth-integrated dissipation (*e.g.,* Trowbridge and Elgar, 2001), particularly as ϵ co-varies across the array (Fig. 2). Therefore the balance $\int h\epsilon \,\mathrm{d}x = cF_{x_{\mathrm{F7}}}$ (similar to Eq. 8) is examined where c is a fit constant of proportionality.

Due to data gaps, $\int_0^{x_\mathrm{b}} h\epsilon \,\mathrm{d}x$ is calculated in two manners: The first only estimates the integral when all surfzone frames have good ϵ estimates resulting in $N = 143$ data points. The second requires at least 2 (for x_b at F3 or F4) or 3 (for x_b at F5 or F6) good surfzone ϵ to calculate the integral resulting in $N = 430$ data points.

The integrated surfzone dissipation $\int_0^{x_\mathrm{b}} h\epsilon \,\mathrm{d}x$ using either estimator is linearly related to the incoming wave energy flux $F_{x_{\mathrm{F7}}}$ (Fig. 2), demonstrating the link between incoming wave energy and viscous dissipation to heat, but $\int_0^{x_\mathrm{b}} h\epsilon \,\mathrm{d}x$ is two orders of magnitude smaller than $F_{x_{\mathrm{F7}}}$ (Fig. 2). With the first $\int_0^{x_\mathrm{b}} h\epsilon \,\mathrm{d}x$ estimate ($N = 143$), the relationship between $F_{x_{\mathrm{F7}}}$ and $\int_0^{x_\mathrm{b}} h\epsilon \,\mathrm{d}x$ has moderately high squared correlation $r^2 = 0.61$ with least-squares best-fit slope of $c = 0.01$ (Fig. 2a), indicating that only 1% of the depth-normalized wave energy is observed. Using the second $\int_0^{x_\mathrm{b}} h\epsilon \,\mathrm{d}x$ estimator, with $3\times$ the number of good data points ($N = 430$), the relationship is similar, but noisier, with squared correlation $r^2 = 0.35$ and slope of $c = 0.008$ (Fig. 2b). For more details please see *Feddersen* (2011).

Episodic Nutrient Fluxes and Phytoplankton Modeling

Here, we estimate the vertical advective and turbulent nitrate fluxes during brief (< 1 week) pulses of $\mathrm{NO_3}$ to the nearshore euphotic zone in 18 m water depth, between mid-June and mid-October 2006, at Huntington Beach, CA. A nearby $\mathrm{Chl}\,a$ timeseries chronicles the rapid growth and decline of three distinct phytoplankton blooms, one of which was a red tide of the dinoflagellates *Lingulodinium polyedrum*. We use temperature as a proxy for $\mathrm{NO_3}$, and inferred the episodic turbulent, and advective fluxes from water column measurements of currents and temperature. Each $\mathrm{NO_3}$ flux event preceded a bloom event, indicating that blooms may be a response to these fluxes. The correlation between the $\mathrm{NO_3}$ flux and the observed $\mathrm{Chl}\,a$ was maximum ($r^2 = 0.40$) with an 8 day lag. A simple local Nitrate-Phytoplankton (NP) model using a linear uptake function and driven with the $\mathrm{NO_3}$ flux captured the timing, magnitude, and duration of the three $\mathrm{Chl}\,a$ blooms (skill$= 0.61$) using optimal net growth rate parameters that were within the expected range

(Figure 3). The success of a very simple 2 parameter NP model in reproducing the fundamental features of all three blooms are included) highlights the strong connection between the vertical nitrate flux and the lagged Chl *a* response, and may assist the design of future nearshore programs identify the critical physical parameters and timescales to gain a potentially predictive insight into bloom dynamics in Southern California. For more details please see *Omand et al.* (2011b).

IMPACT/APPLICATIONS

Potential impacts include improving surfzone and nearshore mixing parameterizations based upon bulk factors such as wave height, wave period, bathymetry, and currents.

RELATED PROJECTS

The Tidal-Inlets/River-Mouths DRI project is building upon the dye tracer and drifter results here, but with expanded geographical scope to include a tidal inlet.

References

Boehm, A. B., S. B. Grant, J. H. Kim, C. D. McGee, S. Mowbray, C. Clark, D. Foley, and D. Wellmann, Decadal and shorter period variability of surfzone water quality at Huntington Beach, California. *Environ. Sci. Technol.*, *36*, 3885–3892, 2002.

Clark, D. B., F. Feddersen, M. M. Omand, and R. T. Guza, Measuring fluorescent dye in the bubbly and sediment laden surfzone, *Water Air Soil Poll.*, doi: 10.1007/s11270-009-0030-z, 2009a.

Clark, D. B., F. Feddersen, and R. T. Guza, Cross-shore surfzone tracer dispersion in an alongshore current, *J. Geophys. Res.*, *115*, doi:10.1029/2009JC005683, 2010.

Clark, D. B., F. Feddersen, and R. T. Guza, Modeling Surfzone Tracer Plumes, Part 2: Transport and Dispersion, *J. Geophys. Res.,* , in press, 2011.

Feddersen, F., Trowbridge, J. H., and Williams, A. J., 2007: Vertical structure of dissipation in the nearshore. *J. Phys. Ocean.*, *37*, 1764–1777.

Feddersen, F., Quality Controlling Surfzone Acoustic Doppler Velocimeter Observations to Estimate the Turbulent Dissipation Rate, *J. Atmospheric Oceanic Tech.*, in press, 2010.

Feddersen, F., Observations of the Surfzone Turbulent Dissipation Rate, *J. Phys. Oceangr.,* , in press, 2011.

Feddersen, F., D. B. Clark, and R.T. Guza, Modeling Surfzone Tracer Plumes, Part 1: Waves, Mean Currents, and Low-frequency Eddies, *J. Geophys. Res.,* , in press, 2011.

George, R., R. E. Flick, and R. T. Guza, Observations of turbulence in the surf zone. *J. Geophys. Res.*, *99*, 801–810, 1994

Oltman-Shay, J., Howd, P. A., and W. A. Birkemeier, Shear instabilities of the mean longshore current, 2. Field data. *J. Geophys. Res., 94*, 18,031–18,042, 1992

Omand, M., F. Feddersen, D. B. Clark, P. J. S. Franks, J. J. Leichter, and R. T. Guza, The influence of bubbles and sand on chlorophyll fluorescence measurements in the surfzone, *Limnology and Oceanography Methods*, *7*, 354-362, 2009.

Omand, M. O., J. J. Leichter, P. J. S. Franks,, and R. T. Guza, A. J. Lucas, and F. Feddersen, Physical and Biological Processes Underlying the Sudden Appearance of a Red-tide Surface Patch in the Nearshore, *Limnology and Oceanography*, *56*, 787–801, 2011a.

Omand, M. O., P. J. S. Franks, R. T. Guza, and F. Feddersen, Episodic vertical nutrient fluxes and nearshore phytoplankton blooms in Southern California, *Limnology and Oceanography: Fluids*, submitted, 2011b.

Peregrine, D., Surf zone currents. *Theor. Comput. Fluid Dyn.*, *10*, 295–309, 1998.

Spydell, M. S., F. Feddersen, and R. T. Guza, Observations of drifter dispersion in the surfzone: The effect of sheared alongshore currents, *J. Geophys. Res.*, *114*(C07028), doi: 10.1029/2009JC005328, 2009.

Spydell, M., and F. Feddersen, The effect of a finite Lagrangian time-scale on shear dispersion, *J. Fluid Mech.*, in press, 2011.

Spydell, M., and F. Feddersen, A Stochastic Model of Surfzone Drifter Dispersion, in preparation for *J. Geophys. Res.,* , 2011.

Trowbridge, J., and S. Elgar, Turbulence measurements in the surf zone. *J. Phys. Ocean.*, *31*, 2403–2417, 2001.

PUBLICATIONS

Recent publications acknowledging ONR support during this support period can be downloaded at *http://iod.ucsd.edu/∼falk/papers.html* and incude.

- Clark, D. B., F. Feddersen, R. T. Guza, Cross-shore Surfzone Tracer Dispersion in an Alongshore Current, *J. Geophys. Res.,* **115**, C10035, doi:10.1029/2009JC005683m, 2010.

- Feddersen, F., Quality Controlling Surfzone Acoustic Doppler Velocimeter Observations to Estimate the Turbulent Dissipation Rate, *J. Atmospheric Oceanic Tech.*, **27**, 2039–2055, 2010.

- Omand, M. M., J. J. Leichter, R. T. Guza, P. J. S. Franks, A. J. Lucas, and F. Feddersen, Physical and biological processes underlying the sudden appearance of a red-tide surface patch in the nearshore, *Limnology and Oceanography*, **56**, 787-801, 2011.

- Feddersen, F., D. B. Clark, and R.T. Guza, Modeling Surfzone Tracer Plumes, Part 1: Waves, Mean Currents, and Low-frequency Eddies, *J. Geophys. Res.,* , in press, 2011.

- Clark, D. B., F. Feddersen, and R. T. Guza, Modeling Surfzone Tracer Plumes, Part 2: Transport and Dispersion, *J. Geophys. Res.,* in press, 2011.

- Spydell, M. S. and F. Feddersen, The effect of a non-zero Lagrangian time-scale on bounded shear dispersion, *J. Fluid Mech.*, in press, 2011.

- Feddersen, F., Observations of the Surfzone Turbulent Dissipation Rate , *J. Phys. Oceangr.,* in press, 2011.

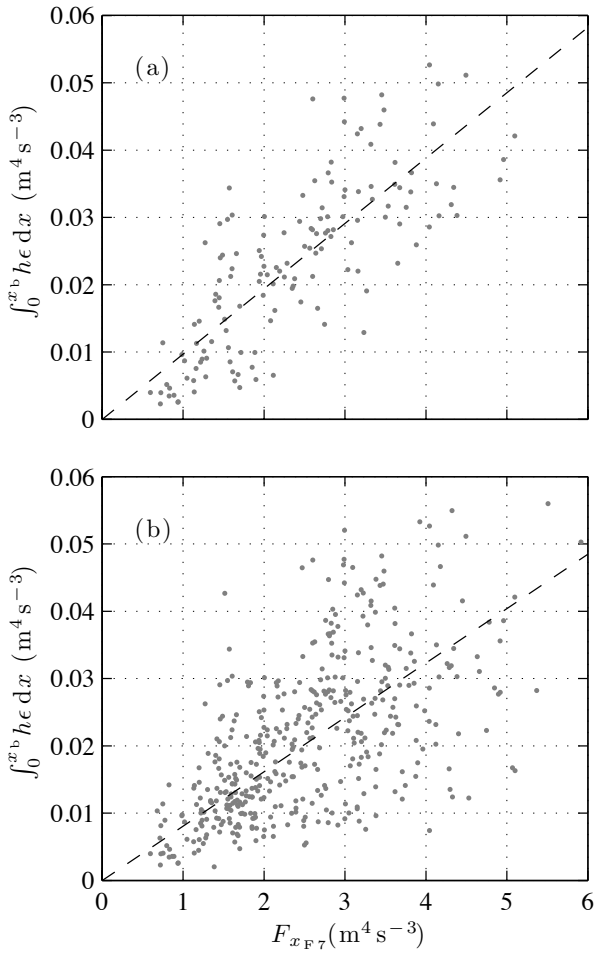

Figure 2: Cross-shore integrated energy balance: $\int_0^{x_b} h\epsilon \, dx$ versus incident F7 wave energy flux $F_{x_{F7}}$ for $\int_0^{x_b} h\epsilon \, dx$ calculated when (a) all surfzone ϵ are good ($N = 143$) and (b) at least 2 (x_b at F3 or F4) or 3 (if x_b is at F5 or F6) surfzone ϵ are good ($N = 430$). The black dashed line represents the least-squares best-fit constrained to go through the origin with the best-fit slope c and squared correlation r^2 of (a) $c = 0.01$ and $r^2 = 0.61$ and (b) $c = 0.008$ and $r^2 = 0.35$, respectively.

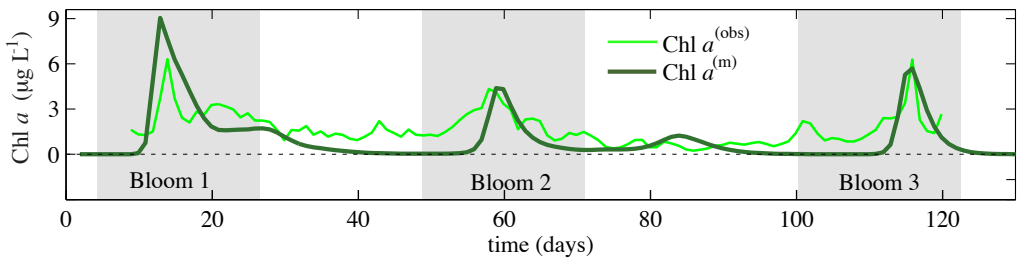

Figure 3: Timeseries of 24 h averaged observed $\mathrm{Chl}\,a^{(\mathrm{obs})}$ ($\mu\mathrm{g}\,\mathrm{L}^{-1}$, light green line) and modeled $\mathrm{Chl}\,a^{(\mathrm{m})}$ ($\mu\mathrm{g}\,\mathrm{L}^{-1}$, dark green line) Chlorophyll-a. The gray shaded regions indicate the time periods of the 3 bloom events.